

**DYNAMICS OF AUTOMATIC COMPRESSOR VALVES UNDER
TURBULENT FLOW CONDITION****F. F. S. Matos**

Empresa Brasileira de Compressores S/A - EMBRACO
Caixa Postal 91, 89219-901, Joinville, SC, Brazil
fred@nrva.ufsc.br

A. T. Prata

Universidade Federal de Santa Catarina, Departamento de Engenharia Mecânica
88040-900, Florianópolis, SC, Brazil.
prata@nrva.ufsc.br

C. J. Deschamps

Universidade Federal de Santa Catarina, Departamento de Engenharia Mecânica
88040-900, Florianópolis, SC, Brazil.
deschamps@nrva.ufsc.br

***Abstract.** This work presents the modeling of automatic compressor valves under turbulent flow condition. The valve dynamics and the time dependent flow field are coupled and therefore solved simultaneously. A system with one-degree of freedom is adopted for the valve motion whereas the turbulent flow is solved with the RNG $k-\epsilon$ model of Orzag et al. (1993), due to its capability to predict complex flow features such as those found in valves. In order to maintain the computational effort within available resources, the flow is considered to be incompressible, isothermal and axisymmetric. A numerical technique has been especially developed to take into account the time variation of the computational domain originated by the valve motion. Through a coordinate transformation a moving coordinate system is obtained so as to expand and contract according to the valve displacement. Results for flow quantities (streamline, turbulence intensity and length scale) and for the valve dynamics (resultant force and displacement) are obtained for a prescribed periodic mass flow rate at the valve entrance.*

Keyword: Automatic valves, compressor valves, turbulence modeling

1. Introduction

In most hermetic reciprocating compressors adopted in household refrigeration the valves are automatic, in the sense that they open and close depending on the pressure difference between the cylinder and suction and discharge chambers. Such valve systems are designed so as to guarantee fast response, large mass flow rate, low pressure drop when opened and good blockage when closed. These performance features are to a great extent affected by the flow through the valve and therefore a good understanding of parameters affecting the valve dynamics and its associated flow is required.

The basic aspects related to the valve dynamics can be explained through Fig. (1), where a reciprocating compressor and a discharge valve are shown schematically. As can be seen, the discharge valve is reed represented by a circular disk parallel to the seat. In this type of valve the unequal pressure distribution acting on both sides of the reed is responsible for opening the valve and as a consequence for generating the flow. As illustrated in the figure, the fluid enters the valve axially through the feeding orifice and then due to the presence of the reed it is forced to flow radially for the rest of the valve passage. The pressure difference between the orifice entrance and the discharge chamber together with the valve lift govern the fluid flow throughout the valve. On the other hand, the flow dictates the pressure distribution on the reed surface and, consequently, the resultant force that will govern the valve dynamics and its displacement from the seat.

Valve performance is a result of a very intricate problem where fluid mechanics and solid dynamics play a definite role. Some recent investigations on valve modeling and radial flows are those by Deschamps et al. (1996), Lopes and Prata (1997), Ezzat Khalifa and Liu (1998), Salinas-Casanova et al. (1999), Matos et al. (2000) and Myung and Lee (2000). Most works related to reed valves either model the valve dynamics in detail but pay little attention to the description of the flow field, or focus on the fluid mechanics without considering the coupling between valve motion and pressure distribution on the reed.

Deschamps et al. (1996) provided an experimentally validated numerical analysis of turbulent flow in reed type valves for the idealized radial diffuser geometry. The RNG k- ϵ model of Orzag et al (1993) was applied in the analysis and the governing equations were solved using the finite volume methodology. Results for pressure distribution on the reed surface when compared to experimental data showed that the RNG k- ϵ model can predict important parameters required for valve design.

Salinas-Casanova et al. (1999) extended the work of Deschamps et al. (1996) so as to include in the analysis the effect of the reed inclination with respect to the seat. Comparisons between numerical results and experimental data demonstrated that the RNG k- ϵ model is able to predict also this more complex class of flow.

Lopes and Prata (1997) considered for the first time a numerical methodology to explore the interaction between valve dynamics and fluid flow. In their work a numerical solution was obtained for the laminar flow with a periodic flow rate prescribed at the feeding orifice entrance. From the pressure distribution on the reed the resultant force was determined and a one-dimensional dynamic model was employed to solve for the reed acceleration, velocity and displacement.

An analytical model to analyze the dynamic behavior of reed valves in the presence of oil was proposed by Ezzat Khalifa and Liu (1998). The authors showed that the primary reason for stiction is the viscous force arising from dilating the oil film between the reed and its seat.

Myung and Lee (2000) used a PIV (Particle Image Velocimetry) system to visualize the discharge flow in a model of reciprocating compressor valve. Fundamental phenomena related to the feeding orifice and the valve were clearly shown in terms of velocity and vorticity fields.

A three-dimensional numerical model to simulate the angular motion of reed type valves was proposed by Matos et al. (2000) for incompressible laminar flow. The velocity field and the resultant force on the reed were obtained for a harmonic motion prescribed to the piston.

The present work prescribes a periodic flow rate through the valve as in Lopes and Prata (1997) but considers the more realistic condition of turbulent flow. To reduce the computational cost, effects of compressibility and heat transfer have been neglected at this stage.

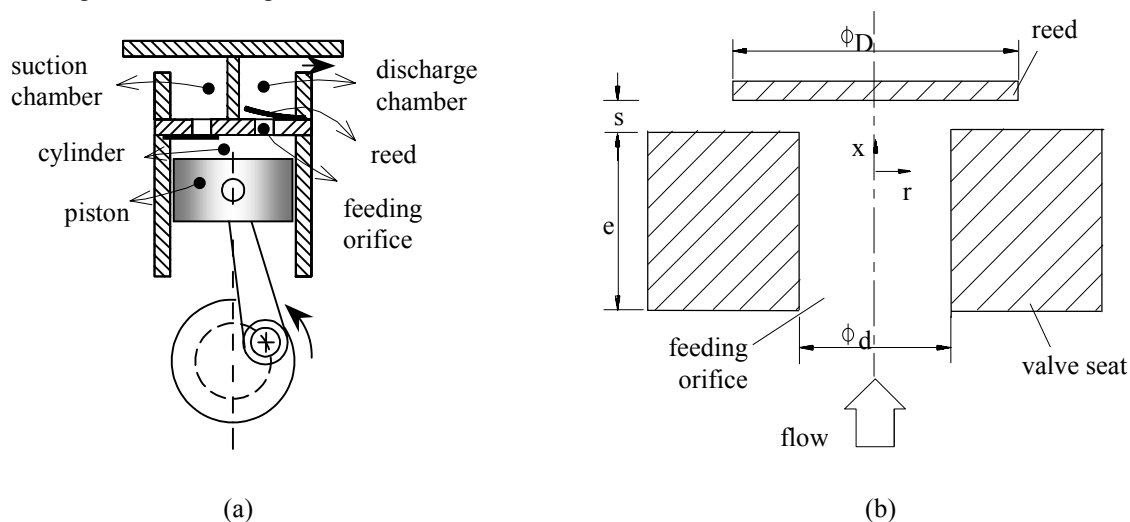


Figure 1. Schematic views of (a) reciprocating compressor (b) reed type valve.

2. Physical models

In the present section, details of the methodologies adopted to model the reed dynamics and the flow through the valve are given. A more comprehensive description is available in Matos (2002).

2.1. Valve dynamics

The dynamics of the reed can be modeled as

$$F - F_0 = m\ddot{s} + C\dot{s} + Ks \quad (1)$$

The reed is assumed to move parallel to the valve seat, with s being the instantaneous valve lift, as shown in Fig. (1b), and \dot{s} and \ddot{s} are the reed velocity and acceleration, respectively. The valve stiffness and damping coefficients, K and C , respectively, as well as the valve mass, m , are determined experimentally. Finally, F_0 is a pre-load force not considered in the present work, but which can be modeled according to the proposal of Ezzat Khalifa and Liu (1998).

The resultant force F on the reed required to solve Eq. (1) is obtained from

$$F = \int_0^{D/2} p \, 2\pi r \, dr \quad (2)$$

where p is the pressure distribution on the reed surface determined from the numerical solution of the flow field.

2.2. Turbulent flow

The axisymmetric flow geometry shown in Fig. (1b) was solved considering the hypothesis of incompressible turbulent flow. The conventional statistical approach for stationary turbulent flow is to decompose the instantaneous flow properties into a time-averaged component and a fluctuating component. Due to the non-stationary character of the flow considered here, an equivalent definition is required and is based on ensemble averaging over a statistically acceptable number of cycles (Arcoumanis and Whitelaw, 1987). The Navier-Stokes equations written for such ensemble-averaged properties are closed using the concept of 'turbulent' or 'eddy' viscosity μ_t . Under the effect of no body force the equations of motion are:

$$\frac{1}{r} \frac{\partial}{\partial r} (\rho r v) + \frac{\partial}{\partial x} (\rho u) = 0 \quad (3)$$

$$\begin{aligned} \frac{\partial}{\partial t} (\rho u) + \frac{\partial}{\partial x} (\rho u u) + \frac{1}{r} \frac{\partial}{\partial r} (\rho r v u) = & -\frac{\partial}{\partial x} \left(p + \frac{2}{3} \rho k \right) + \frac{\partial}{\partial x} \left(\mu_{\text{eff}} \frac{\partial u}{\partial x} \right) + \frac{1}{r} \frac{\partial}{\partial r} \left(r \mu_{\text{eff}} \frac{\partial u}{\partial r} \right) + \\ & + \frac{\partial}{\partial x} \left(\mu_{\text{eff}} \frac{\partial u}{\partial x} \right) + \frac{1}{r} \frac{\partial}{\partial r} \left(r \mu_{\text{eff}} \frac{\partial v}{\partial r} \right) \end{aligned} \quad (4)$$

$$\begin{aligned} \frac{\partial}{\partial t} (\rho v) + \frac{\partial}{\partial x} (\rho u v) + \frac{1}{r} \frac{\partial}{\partial r} (\rho r v v) = & -\frac{\partial}{\partial r} \left(p + \frac{2}{3} \rho k \right) + \frac{\partial}{\partial x} \left(\mu_{\text{eff}} \frac{\partial v}{\partial x} \right) + \frac{1}{r} \frac{\partial}{\partial r} \left(r \mu_{\text{eff}} \frac{\partial v}{\partial r} \right) + \\ & + \frac{\partial}{\partial x} \left(\mu_{\text{eff}} \frac{\partial u}{\partial r} \right) + \frac{1}{r} \frac{\partial}{\partial r} \left(r \mu_{\text{eff}} \frac{\partial v}{\partial r} \right) - \frac{2 \mu_{\text{eff}} v}{r^2} \end{aligned} \quad (5)$$

where $\mu_{\text{eff}} = \mu + \mu_t$ is the effective viscosity, which takes into account the molecular viscosity, μ , and the turbulence viscosity, μ_t . The latter is a measure of the turbulence transport mechanism in comparison with molecular diffusion and is evaluated in terms of the turbulence kinetic energy k and its rate of dissipation ϵ . Following the RNG k - ϵ model of Orzag et al. (1993), the effective viscosity is evaluated as

$$\mu_{\text{eff}} = \mu \left[1 + \left(C_\mu \frac{\rho k^2}{\epsilon \mu} \right)^{1/2} \right]^2 \quad (6)$$

The kinetic energy k and the dissipation ϵ are obtained from their respective modeled transport equations, as follows:

$$\begin{aligned} \frac{\partial}{\partial t} (\rho k) + \frac{\partial}{\partial x} (\rho u k) + \frac{1}{r} \frac{\partial}{\partial r} (\rho r v k) = & \frac{\partial}{\partial x} \left[(\mu + \alpha \mu_t) \frac{\partial k}{\partial x} \right] + \frac{1}{r} \frac{\partial}{\partial r} \left[r (\mu + \alpha \mu_t) \frac{\partial k}{\partial r} \right] + \\ & + \mu_t S^2 - \rho \epsilon \end{aligned} \quad (7)$$

$$\begin{aligned} \frac{\partial}{\partial t} (\rho \epsilon) + \frac{\partial}{\partial x} (\rho u \epsilon) + \frac{1}{r} \frac{\partial}{\partial r} (\rho r v \epsilon) = & \frac{\partial}{\partial x} \left[(\mu + \alpha \mu_t) \frac{\partial \epsilon}{\partial x} \right] + \frac{1}{r} \frac{\partial}{\partial r} \left[r (\mu + \alpha \mu_t) \frac{\partial \epsilon}{\partial r} \right] + \\ & + C_{\epsilon 1} \frac{\epsilon}{k} \mu_t S^2 - C_{\epsilon 2} \frac{\rho \epsilon^2}{k} - \rho R \end{aligned} \quad (8)$$

where C_μ , $C_{\epsilon 1}$ and $C_{\epsilon 2}$ are equal to 0.0845, 1.42 e 1.68; respectively. The inverse Prandtl number, α , for turbulent transport and the rate of strain term, R , are given by the following relationships:

$$\frac{\left| \frac{\alpha - 1.3929}{\alpha_0 - 1.3929} \right|^{0.6321}}{\left| \frac{\alpha + 2.3929}{\alpha_0 + 2.3929} \right|^{0.3679}} = \frac{\mu}{\mu_{\text{eff}}} \quad (9)$$

$$R = \frac{C_\mu \eta^3 (1 - \eta/\eta_0) \varepsilon^2}{1 + \beta \eta^3} k \quad (10)$$

with $\alpha_0 = 1.0$, $\beta = 0.012$, $\eta_0 \approx 4,38$, $\eta = Sk/\varepsilon$ and $S^2 = 2 S_{ij} S_{ij}$ in which S_{ij} is the rate of strain tensor. The term R may change sign depending on whether the time scale ratio η is greater than the value η_0 found in homogenous shear flows. In regions of small strain rate, the term R has a trend to increase μ_{eff} somewhat, whereas in regions of elevated strain rate the sign of R becomes positive and μ_{eff} is considerably reduced. This feature of the RNG k - ε is responsible for substantial improvements verified in the prediction of recirculating flow regions. The smaller value of $C_{\varepsilon 2}$ in the RNG theory compared to other k - ε models acts to increase ε and as a consequence to diminish μ_t .

Equations (1)-(10) completely describe the problem and seven unknowns are to be determined: s , F , u , v , p , k and ε . Concerning boundary conditions, at the solid walls all velocity components are zero with the exception of the reed surface. There, the radial component, v , is zero but the axial velocity corresponds to the reed velocity \dot{s} , which is obtained from Eq. (1). The symmetry conditions at the valve axis implies that $v = \partial u/\partial r = 0$. The computational domain was extended well beyond the valve exit and there a pressure boundary condition was prescribed. More details on the implementation of this type boundary condition can be found in Versteeg and Malalasekera (1995).

No information is available for turbulence kinetic energy at the inlet boundary. However, numerical tests have shown that when the level of the turbulence intensity

$$I = \frac{\sqrt{2k/3}}{U_{\text{in}}} \quad (11)$$

is increased from 3% to 6% no significant change occurs in the predicted flow. A value of 3% was used in the calculation of all results shown in this work. The dissipation rate at the entrance was estimated based on the assumption of equilibrium boundary layer, that is

$$\varepsilon = \lambda^{3/4} k^{3/2} / \ell_m \quad (12)$$

where $\ell_m = 0.07d/2$ and $\lambda = 0.09$.

At the solid boundaries, the turbulence kinetic energy k was set to zero and for the dissipation ε , rather than being prescribed at the walls, its value was calculated in the control volume adjacent to the wall following a non-equilibrium wall-function.

3. Solution methodology

A key issue in solving the governing equations is the required methodology to handle the physical domain that expands and contracts as the reed moves up and down, respectively. Following the practice adopted in Cato and Prata (1997), a moving coordinate system was employed, which transforms the physical domain into a computational domain and remains unchanged regardless the reed motion. In this moving coordinate system the axial coordinate, x , of the inertial system is replaced by a new axial coordinate, ξ , using the following transformation,

$$\frac{x(t) - x_s}{x_r(t) - x_s} = \frac{\xi - \xi_s}{\xi_r - \xi_s} \quad (13)$$

where the subscripts s and r represent seat and reed, respectively. The physical and computational domains are both shown in Fig. (2). Because the physical domain is composed of a variable region in the diffuser and a fixed region in the orifice, for computational reasons it was preferred to keep the reed fixed and let the seat move (this makes no difference regarding the physical model).

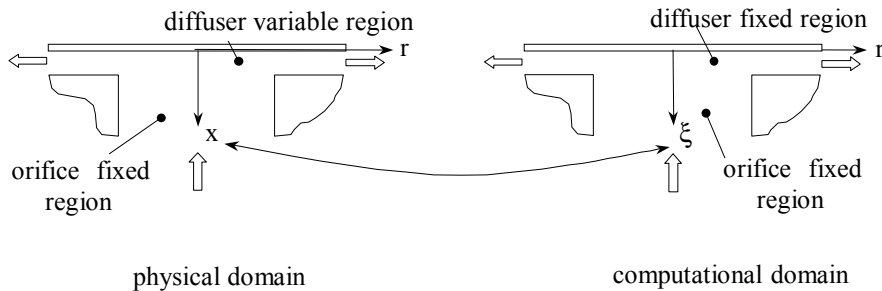


Figure 2. Physical and computational domains.

Transforming the governing equations from the fixed system to the moving system yields

$$\frac{1}{x_r} \frac{\partial (\rho x_r \phi)}{\partial t} + \frac{1}{x_r} \frac{\partial (\rho \tilde{u} \phi)}{\partial \xi} + \frac{1}{r} \frac{\partial (\rho r v \phi)}{\partial r} = \frac{1}{x_r} \frac{\partial}{\partial \xi} \left(\frac{\Gamma_\phi}{x_r} \frac{\partial \phi}{\partial \xi} \right) + \frac{1}{r} \frac{\partial}{\partial r} \left(r \Gamma_\phi \frac{\partial \phi}{\partial r} \right) + S_\phi \quad (14)$$

The transport equation above is written for a generic property (mass, momentum, turbulence kinetic energy and turbulence dissipation). The appropriate ϕ , Γ_ϕ and S_ϕ to each property are shown in Matos (2002). In Eq. (14) the axial velocity \tilde{u} is that corresponding to the moving coordinate, ξ . Once \tilde{u} is determined, the velocity u associated to the inertial system can be obtained from,

$$u = \tilde{u} + u_g \quad (15)$$

where u_g is the instantaneous velocity of the coordinate ξ given by,

$$u_g = \left(\frac{\partial x}{\partial t} \right)_{\xi, r} = \frac{\xi - \xi_s}{\xi_r - \xi_s} \frac{\partial x_r}{\partial t} = \frac{\xi - \xi_s}{\xi_r - \xi_s} u_r \quad (16)$$

in which $u_r = \dot{s}$ is the instantaneous reed velocity.

The numerical solution of the governing equations was performed using a finite volume methodology. For this practice the solution domain is divided in small control volumes, using a staggered grid scheme, and the governing differential equations are integrated over each control volume with the use of Gauss's theorem. In the present work, the QUICK scheme was adopted in the solution of the momentum equations (Hayase et al., 1992). Yet, for the transport equations of turbulence quantities the Power Law Differencing Scheme (PLDS) was adopted since the unboundedness of the QUICK scheme usually introduces serious numerical instabilities. Nevertheless, there is some evidence that in the case of these equations the source terms are dominant, with the convective terms playing a secondary role.

A segregated approach was employed to solve the equations and the coupling between pressure and velocity was handled through the SIMPLEC algorithm. A fully implicit scheme was adopted to discretize the unsteady terms.

The solution domain had 37 x 32 (axial x radial) grid points in the orifice region and 33 x 80 grid points (axial x radial) in the region between the reed and the valve seat. A more refined grid was not feasible due to the already extremely high computational cost required for the solution. However, the grid employed in the computations was successful in capturing the main features of the flow field as will be discussed shortly in the presentation of numerical results.

An interval of $2\pi/(360\omega)$ was employed for the time step, with $\omega = 2\pi f$ [rad/s]. The differential equation governing the valve motion, Eq. (1), was solved analytically considering the resultant force on the reed to be constant during each time step.

4. Results and discussion

The first step in the numerical analysis was to validate the computational code written for a moving coordinate system. Ishizawa et al. (1987) obtained experimental results for the flow laminar through a radial diffuser with a geometry very similar to the one investigated here, except that in their work the diameter ratio was $D/d = 10$, which is much larger than typical values of compressor valves. A constant mass flow rate was set at the feeding orifice and a time varying gap between the disks representing the seat and the reed was externally imposed as follows:

$$\frac{s(t)}{d} = \frac{\bar{s}}{d} [1 + A \sin(\omega t)] \quad (17)$$

where A is the amplitude and ω is the angular frequency. The resultant axial force on the frontal disk (reed) was measured using a load cell.

Flow rate and frequency associated to the flow are expressed through the following Reynolds number definitions:

$$R_\omega = \frac{\bar{s}^2 \omega}{\nu} \quad (18)$$

$$R_q = \frac{4\bar{s}q_s}{\nu D^2} \quad (19)$$

with ν being the fluid kinematics viscosity and $q_s = q/2\pi$ a measure of the flow rate at the feeding orifice.

The flow geometry chosen for the simulation had $d = 0,03\text{m}$, $e/d = 1$, $D/d = 10$, $\bar{s}/d = 1/15$ and the working fluid was air ($\mu = 1.8 \times 10^{-5} \text{ Pa}\cdot\text{s}$ and $\rho = 1.2 \text{ kg/m}^3$). Values for frequency ω e flow rate q_s required to complete the formulation can be evaluated from the Reynolds numbers R_q e R_ω , as given by Eqs. (18) e (19).

In Fig. (3) experimental data of Ishizawa et al. (1987) for dimensionless force $F^* [= F (2 \bar{s}/D)^4 / (\rho v^2)]$ are compared with numerical results obtained with the present methodology. In the experiment the gap between the disks is much smaller than the diffuser length and an analytical solution, also indicated in Fig. (3), can be obtained. The good agreement between experimental, numerical and analytical results yielded confidence on the present numerical methodology.

The next step was to solve the reed dynamics coupled with the flow field through the valve. A crucial aspect of numerical flow simulation in compressor valves is that related to turbulence modeling. A number of works have examined different approaches to predict the main flow features in valves (see for instance Deschamps et al., 1996 and Salinas-Casanova et al, 2000) and concluded that the RNG k- ϵ model is best option. Therefore, this model has been adopted here.

For all results to be presented, the main geometric parameters are the reed diameter D ($= 9.0 \text{ mm}$), the orifice diameter d ($= 6.0 \text{ mm}$) and the orifice length e ($= 1.6 \text{ mm}$). The valve parameters used in Eq. (1) are $K = 200 \text{ N/m}$, $C = 0.5 \text{ N s/m}$, $m = 3.2 \text{ g}$ and $F_0 = 0$. In line with actual compressor discharge systems, a stopper was included in the computational model to limit the opening of the valve and positioned at $s/d = 0,166$.

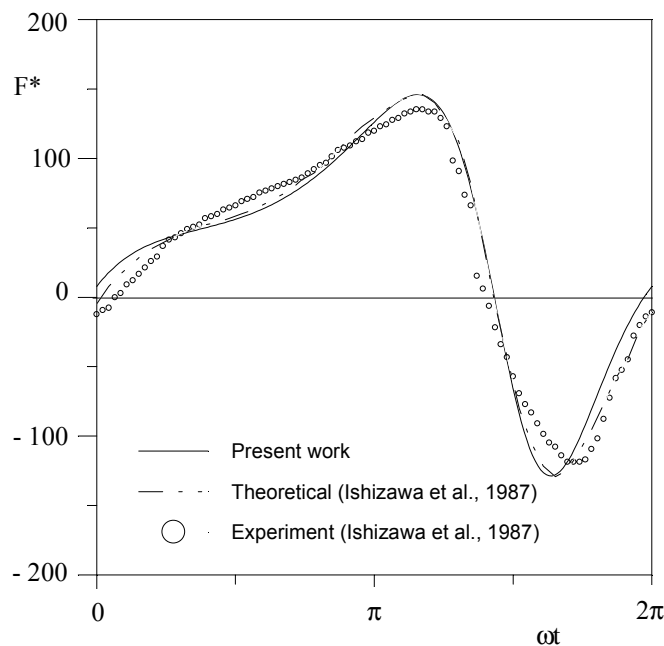


Figure 3. Dimensionless force acting on the reed for a prescribed time varying valve lift: $R_\omega=20,05$, $R_q=0,88$ e $A=0,43$.

Actually, the flow rate through the valve is a function of the instantaneous pressure drop between the cylinder and the discharge chamber. Here instead, the flow rate is set to vary harmonically according to the following expression for the Reynolds number:

$$\text{Re}(t) = \overline{\text{Re}} [1 + 0.9 \sin(\omega t)] \quad (20)$$

with $f = 60 \text{ Hz}$ and $\overline{\text{Re}} = 25,000$. The Reynolds number Re is defined with reference to the feeding orifice, i.e. $\text{Re} = \rho U_{in} d / \mu$. A pressure boundary condition equal to $1.0 \times 10^5 \text{ Pa}$ was prescribed at the discharge chamber.

Results for valve lift and resultant force on the reed are presented in Fig. (4) as a function of time. For reference, in that figure is also shown the instantaneous Reynolds number prescribed at the valve feeding through Eq. (20). The figure shows that large mass flow rates bring about large values of resultant forces and valve lifts, as would be expected, and the exact moment when the reed reaches its maximum displacement. A very useful information that can be provided by the present model is the velocity with which the reed hits the stopper.

Figure (4) also shows a decrease in the resultant force just before the reed reaches the stopper and the local minimum then originated. This can be explained with reference to dimensionless streamlines Ψ^* ($= \Psi / \dot{m}$) in Fig. (5) and dimensionless pressure distributions P^* ($= p / (\rho v^2 / 2)$) on the reed in Fig. (6) for $\omega t = 4\pi/180$, $20\pi/180$, $25\pi/180$, $39\pi/180$ and $45\pi/180$. Such time positions are identified in Fig. (4) by letters **a**, **b**, **c**, **d** and **e**, respectively. As can be seen in Fig. (6), the presence of the reed creates a plateau on the central part of the pressure distribution ($r/d < 0.5$), whereas the sharp pressure drop at the radial position $r/d \approx 0.5$ is associated with both the change in the flow direction

and the reduction in the flow passage area. The latter is particularly strong in the range of valve lift and Reynolds number considered here since a recirculating flow region is always present on the valve seat; see Fig. (5). The associated reduction in the flow passage area causes an increase in velocity and a decrease in pressure. After reaching a condition of minimum, the pressure level on the reed is increased as the flow progresses towards the valve exit. It is interesting to note that in all situations shown in Fig. (6) the pressure at the exit of the valve is higher than the pressure in the discharge chamber.

The dimension h indicated in Fig. (4d) is a measure of the minimum flow passage area related to the recirculating region. For $\omega t = 4\pi/180$ in Fig. (4a) this minimum occurs at $r/d = 0.635$ ($h = 0.30$ mm) and originates the minimum in the pressure distribution shown in Fig. (6). As the reed moves from locations **a** to **b** in the cycle, the recirculating flow region becomes larger, but the height h is also increased ($h = 0.38$ mm) and the radial position for the minimum passage area happens at $r/d = 0.678$. This originates a smaller pressure drop on the reed surface and an increase in the resultant force.

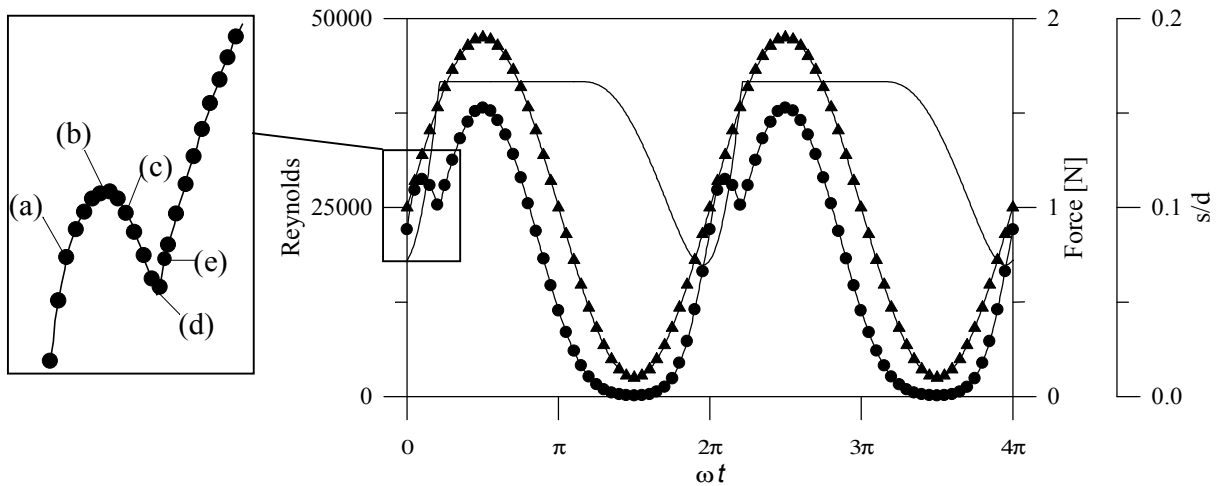


Figure 4. Valve lift and resultant force on the reed in response to periodic mass flow rate.

▲ Reynolds, ● Force, — s/d.

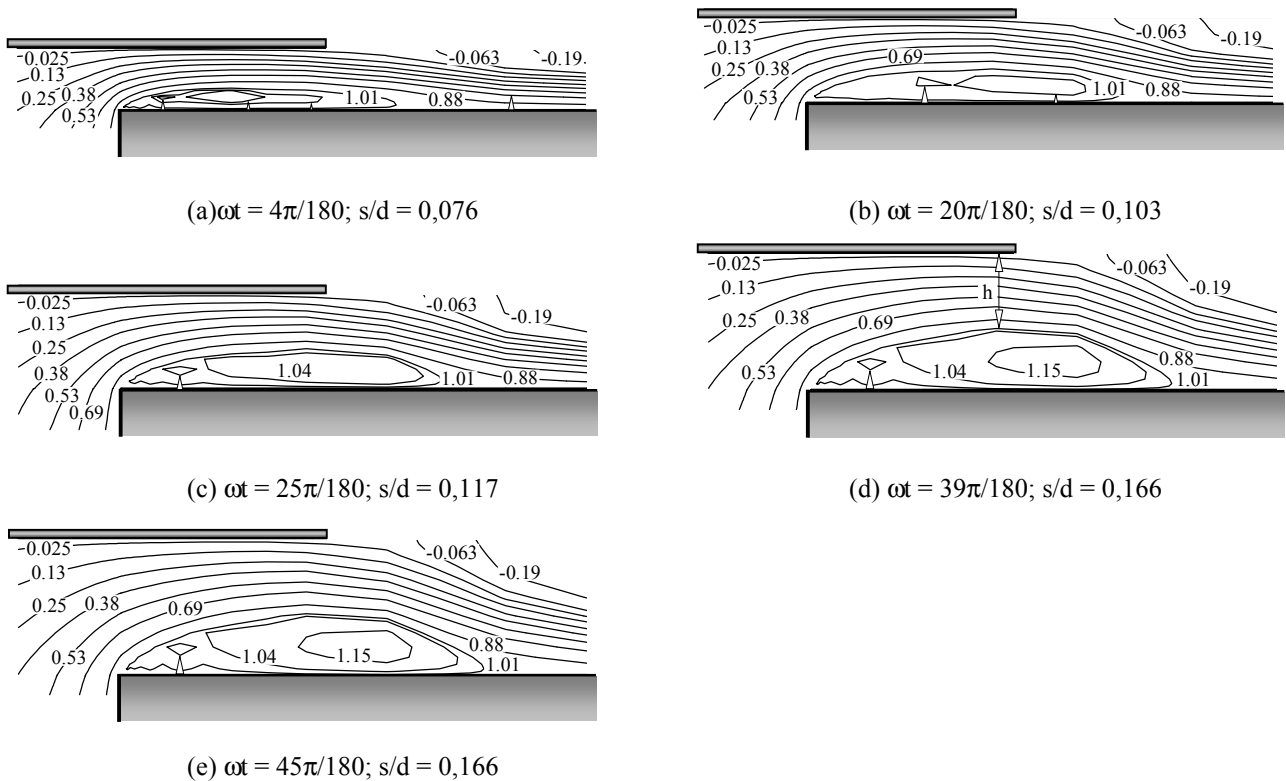


Figure 5. Dimensionless streamlines Ψ^* ($=\Psi/\dot{m}$).

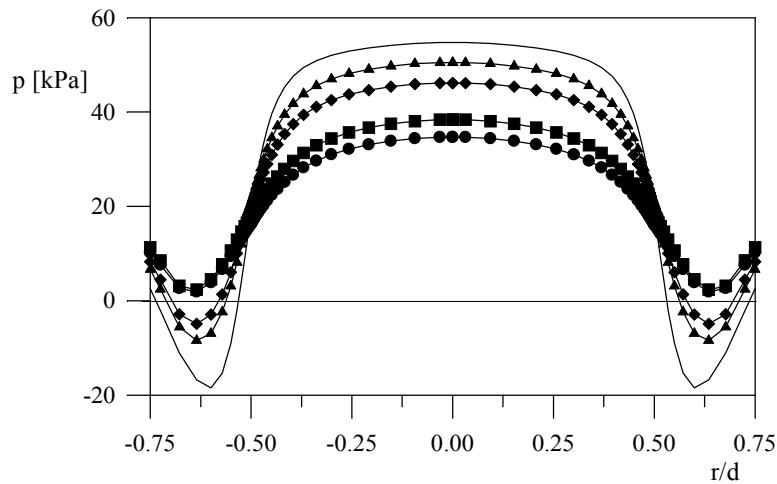


Figure 6. Pressure distribution on the reed as the maximum lift is reached.

- $\omega t = 4\pi/180$, $Re = 26570$, $F = 1.007$ N
- $\omega t = 20\pi/180$, $Re = 32700$, $F = 1.151$ N
- ◆ $\omega t = 25\pi/180$, $Re = 34860$, $F = 1.127$ N
- $\omega t = 39\pi/180$, $Re = 39160$, $F = 1.007$ N
- $\omega t = 45\pi/180$, $Re = 40910$, $F = 1.117$ N

As can be seen in Fig. (4c) for $\omega t = 25\pi/180$, as the valve opens the height h is increased even further ($h = 0.41$ mm) despite the presence of a larger recirculating flow region. This acts to lessen the negative pressure region on the reed surface but because the pressure level in the stagnation region ($r/d < 0.5$) becomes smaller (Fig. (6)), the overall result is a reduction in the resultant force (Fig. (4)). A similar reduction in the force takes place for $\omega t = 39\pi/180$, point **d** in Fig. (4), at the exact moment when the reed hits the stopper and $h = 0.56$ mm.

Finally, for $\omega t = 45\pi/180$ (point **e** in Fig. (4)), the reed is totally open for some time and a flow configuration virtually identical to that for $\omega t = 39\pi/180$ is verified, with $h = 0.55$ mm. In spite of that and because the mass flow rate (represented by the Reynolds number) is increasing, the pressure level in the stagnation region becomes larger (Fig. (6)) and the same occurring with the resultant force.

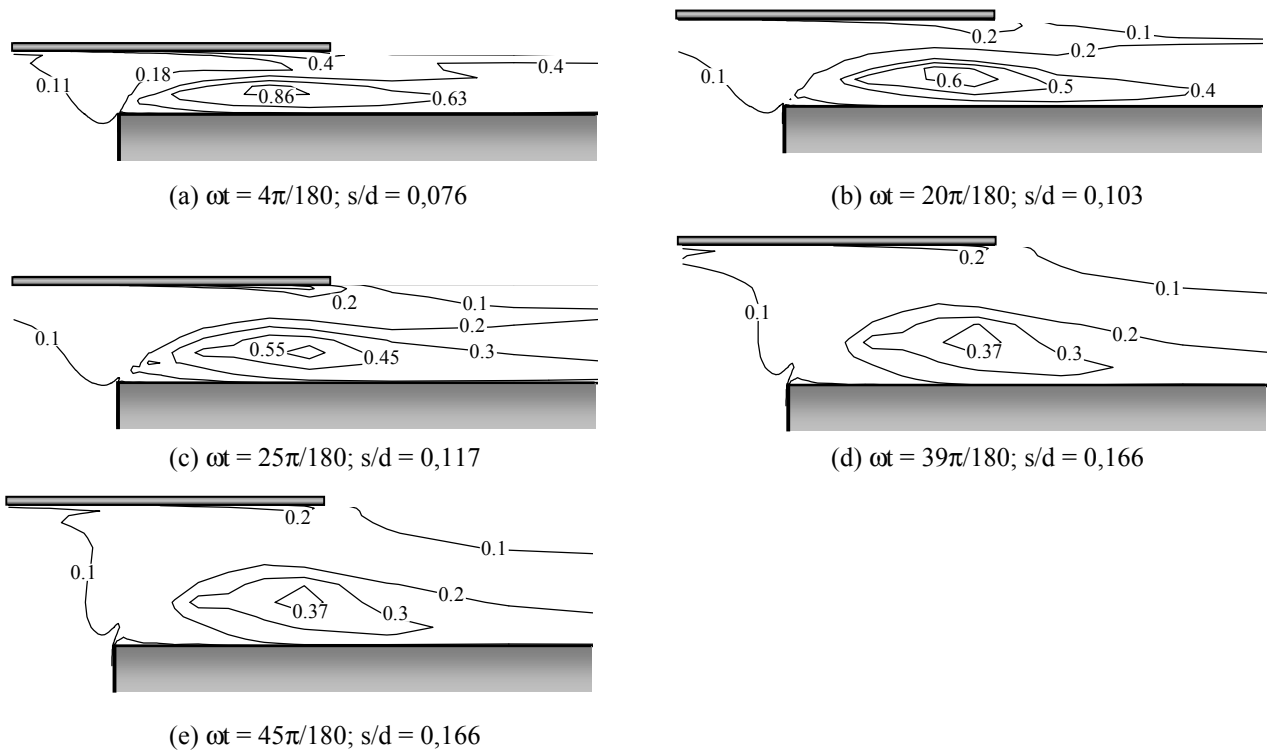


Figure 7. Turbulent Intensity $I (= [2k/3]^{1/2} / U_{in})$.

Results for turbulence intensity $I (= [2k/3]^{1/2}/U_{in})$ contours are presented in Fig. (7) for time positions ωt considered above. A common feature in all valve lifts is the high level of turbulence generated by the recirculating flow regions. On the other hand, the decrease in the intensity observed for large valve lifts is a result of smaller strain rates due to larger flow passage areas. Fig. (8) shows estimates for dimensionless length scale $L (= k^{3/2}/\epsilon)$. As one can see, levels of L are physically consistent if compared with values of valve lifts s/d indicated in Fig. (8). A more complete analysis of turbulence quantities would require further experimental evidence, which is not available at the present.

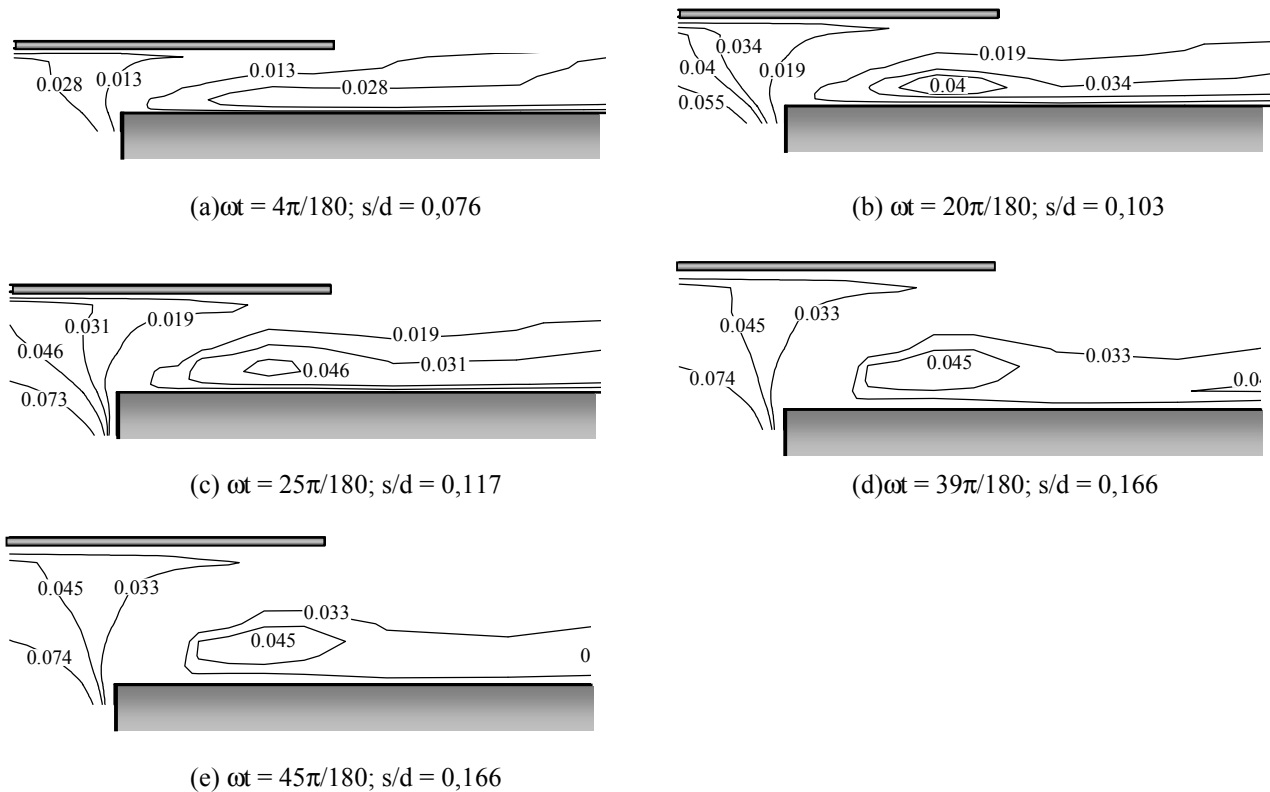


Figure 8. Dimensionless length scales $L (= k^{3/2}/\epsilon)$.

5. Conclusions

The present work considered the modeling of the dynamics of automatic valves commonly adopted in reciprocating compressors. The complex interaction between reed dynamics and gas flow was incorporated into the physical and mathematical models. Because the main focus of the work is to develop a numerical methodology to solve for the reed dynamics, at this stage a simple periodic flow rate condition was set at the valve entrance. The present methodology is capable of capturing some characteristics found in the dynamics of actual valves, such as the impact against the stopper for conditions of large mass flow rates. Despite some important insights provided by the present analysis, the work has to be extended so as to take into account important flow features found in compressor valves, such as compressibility effects. Additionally, the flow rate through the valve should be expressed as a function of instantaneous pressure drop between the cylinder and the discharge chamber.

6. Acknowledgments

The present work is part of a technical-scientific program between Federal University of Santa Catarina and EMBRACO S/A. Support from the Brazilian Research Council, CNPq, is also appreciated.

7. References

- Arcoumanis, C. and Whitelaw, J.H., 1987, "Fluid Mechanics of Internal Combustion Engines – A Review", Proc. Instn. Mech. Engrs., Vol. 201, No. C1, UK, pp. 57-74.
- Catto, A.G. and Prata, A.T., 1997, "A Numerical Study of Instantaneous Heat Transfer During Compression and Expansion in Piston-Cylinder Geometry", AES-Vol. 37, Proc. ASME Advanced Energy System Division, Dallas, USA, pp. 441-450.
- Deschamps, C.J., Prata A.T. and Ferreira, R.T.S., 1996, "Turbulent Flow Through Plate Type Valves of Reciprocating Compressors", Proc. ASME Advanced Energy Systems Division, Atlanta, USA, AES-Vol. 36, pp. 151-161.

- Ezzat Khalifa, H. and Liu, X., 1998, "Analysis of Stiction Effect on the Dynamics of Compressor Suction Valve", Proc. International Compressor Engineering Conference at Purdue, West Lafayette, USA, pp. 87-92.
- Hayase, T., Humphrey, J.A.C., and Greif, R., 1992, "A Consistently Formulated QUICK Scheme for Fast and Stable Convergence Using Finite-Volume Iterative Calculation Procedures", Journal of Computational Physics, V. 98, pp. 108-118.
- Ishizawa, S., Watanabe, T. and Takahashi, K., 1987, "Unsteady Viscous Flow Between Parallel Disks with a Time-Varying Gap Width and a Central Fluid Source", ASME Journal of Fluids Engineering, v.109, pp.394-402.
- Lopes, M.N. and Prata, A.T., 1997, "Dynamic Behavior of Plate Type Valves in Periodic Flows" (in portuguese), Proc. XIV Brazilian Congress of Mechanical Engineering (CD-ROM), Bauru, Brazil, COB 1138.
- Matos, F.F.S., 2002, "Numerical Analysis of the Dynamic Behavior of Reed Type Valves in Reciprocating Compressors" (in Portuguese), Ph.D. Thesis, Federal University of Santa Catarina, Brazil.
- Matos, F.F.S., Prata, A.T., Deschamps, C.J., 1999, "Numerical Analysis of the dynamic behaviour of plate valves in reciprocating compressors", Proc. International Conference on Compressor and their Systems, London, UK, pp. 453-462.
- Matos, F.F.S., Prata, A.T. and Deschamps, C.J., 2000, "A Numerical Methodology for the Analysis of Valve Dynamics", Proc. Compressor Engineering Conference at Purdue, West Lafayette, USA, pp. 383-390.
- Myung, H.J. and Lee, I.S., 2000, "Investigation of the Discharge Flow of a Reciprocating Compressor using PIV", Proc. Compressor Engineering Conference at Purdue, West Lafayette, USA, pp. 391-396.
- Orzag, S.A., Yakhot, V., Flannery, W., Boysan, F., Choudhury, D., Marusewski, J., Patel, B., 1993, "Renormalization Group Modeling and Turbulence Simulations", Near-wall Turbulent Flows, Elsevier Science Publisher.
- Salinas-Casanova, D.A., Deschamps, C.J., Prata, A.T., 1999, "Turbulent Flow Through a Valve with Inclined reeds", International Conference on Compressor and their Systems, London, UK, pp. 443-452.
- Versteeg, H. K. and Malalasekera, W., 1995, "An Introduction to Computational Fluid Dynamics", Longman Scientific & Technical.